

Drag-Tracking Guidance for Entry Vehicles Without Drag Rate Measurement*

Han Yan[†] and Yingzi He[‡]

Science and Technology on Space Intelligent Control Laboratory,
Beijing Institute of Control Engineering, Beijing 100190, China

Abstract: A robust entry guidance law without drag rate measurement is designed for drag-tracking in this paper. The bank angle is regarded as the control variable. First, a state feedback guidance law (bank angle magnitude) that requires the drag and its rate as feedback information is designed to make the drag-tracking error be input-to-state stable (ISS) with respect to uncertainties. Then a high gain observer is utilized to estimate the drag rate which is difficult for a vehicle to measure accurately in practice. Stability analysis as well as simulation results show the efficiency of the presented approach.

Key words: Entry vehicle, drag-tracking, input-to-state stability, high-gain observer, robustness.

*This work was supported by the National Nature Science Foundation of China under Grant 61403030.

[†]Engineer, e-mail: yhbice@gmail.com.

[‡]Professor.

1 Introduction

For entry vehicles, guidance algorithm plays an important role in steering the vehicle through the atmospheres safely with mission requirements. In general, guidance methods for entry can be classified into two types: predictor-corrector guidance and reference-trajectory guidance. The main merit of predictor-corrector guidance is that it can update the reference trajectory every guidance period online so as to improve the guidance precision. But computing reference trajectory online is time consuming, so the method may be not feasible in practice. In particular, the performance of predictor-corrector guidance might be degraded if we do not have a good grasp of the atmosphere information (such as the Mars atmosphere), since the scheme relies on the accurate entry dynamics model [1]. The drag acceleration is strongly related to the measurable accelerations, and it further has exact kinematic relationship with the arc length of the flying trajectory [2]. Therefore, the drag profile tracking approach, which is one kind of reference-trajectory guidance, has been validated in the Apollo and Shuttle Programs [3] and extensively investigated, and comparing with the predictor-corrector guidance, the approach has distinct advantages in realization.

The feedback linearization method is a typical tool that was applied in the drag-tracking control [2, 4–7], but the desired asymptotic convergence of the drag tracking error can not be guaranteed in the presence of uncertainties or control saturation. In order to take the control saturation into account, Lu and co-workers [8] solved the tracking control problem for a continuous-time nonlinear system with bounded input by using the continuous-time nonlinear predictive control method, and they applied the approach to drag-tracking problem [9]. In their works, the control was designed to minimize a cost function related to the predicted error. [10]

used a different cost function to design the control law for drag-tracking. Considering the model uncertainties, the guidance law design problem for low-lifting skip reentry subject to control saturation was studied in [11] based on nonlinear predictive control in the case that the number of output variables does not equal the number of input variables. The robust control that was applied to robot manipulators [12] was also adopted for drag-tracking in Mars atmospheric entry flight to make the tracking error converge into a small neighbourhood of zero [1]. Most of drag-tracking guidance laws (e.g. see [1, 2, 9–11]) require the knowledge of drag rate, which is hard for a vehicle to measure accurately in practice. Thus, the altitude rate was used as feedback instead of the drag rate in the Shuttle guidance, but it is error prone as mentioned in [3]. The sliding mode state and perturbation observer (SMSPO) was used in [7] to address the issue of estimation of the drag rate. In [13], the active disturbance rejection control (ADRC) algorithm was utilized to design a drag-tracking law for Mars pinpoint landing, and an extended state observer (ESO) was introduced to estimate the drag rate and an extended state. However, uncertainties were not fully considered in [7, 13], and the stability analysis of the closed-loop system in [13] was not provided. Besides the idea of tracking reference drag, [14] studied the full states trajectory tracking control problem under the multi-constrained conditions by using Legendre pseudospectral feedback method.

In this paper, a robust entry guidance law without drag rate measurement is designed for drag-tracking. First, the drag dynamics with uncertainties is formulated, and a state feedback guidance law (desired bank angle magnitude), which requires the drag and its rate as feedback information, is designed to make the drag-tracking error be input-to-state stable (ISS) with respect to uncertainties. As stated earlier, the drag rate is not feasible to be used as feedback

information, and in view of this, a high-gain observer [15, 16] is integrated into the guidance law to estimate the drag rate, which fulfills the guidance law design without drag rate measurement. Moreover, the stability analysis is provided to show that ISS property of the closed-loop system under the state feedback guidance law can be recovered by using a sufficiently fast high-gain observer.

The remainder of this paper is organized as follows. The drag dynamics is formulated in Section 2. After presenting the state feedback guidance law, the high-gain observer is introduced to estimate the drag rate in Section 3. Section 4 shows the simulation results. Finally, Section 5 summarizes the conclusions.

2 Model Derivation

The motion equations of an unpowered, point mass vehicle flying over a non-rotating planet in a stationary atmosphere are given by [7, 11, 13, 14]

$$\dot{r} = v \sin \gamma \tag{1a}$$

$$\dot{\phi} = \frac{v \cos \gamma \sin \chi}{r \cos \theta} \tag{1b}$$

$$\dot{\theta} = \frac{v \cos \gamma \cos \chi}{r} \tag{1c}$$

$$\dot{v} = -D - g \sin \gamma \tag{1d}$$

$$\dot{\gamma} = \frac{L \cos \sigma}{v} - \left(\frac{g}{v} - \frac{v}{r} \right) \cos \gamma \tag{1e}$$

$$\dot{\chi} = \frac{L \sin \sigma}{v \cos \gamma} + \frac{v \cos \gamma \sin \chi \tan \theta}{r} \tag{1f}$$

where r is the radial position, ϕ is longitude, θ latitude, v is the velocity, γ is the flight path angle, χ is the heading angle, L is the lift acceleration, D is the drag acceleration, and g is gravitational acceleration. L and D can be calculated as

$$L = \frac{1}{2m} \rho v^2 S \underbrace{(C_L^0 + \Delta C_L)}_{C_L} \quad (2a)$$

$$D = \frac{1}{2m} \rho v^2 S \underbrace{(C_D^0 + \Delta C_D)}_{C_D} \quad (2b)$$

where m is the vehicle mass, ρ is the atmospheric density, S is the reference area, C_L^0 and C_D^0 are nominal values of aerodynamic coefficients, and ΔC_L and ΔC_D are bounded uncertainties. An exponential atmospheric density model

$$\rho = \rho_0 e^{-\frac{h}{h_s}} + \Delta \rho \quad (3)$$

is assumed, where $h = r - r_0$, r_0 is the reference radius, ρ_0 is atmospheric density at the reference radius, $\Delta \rho$ is bounded uncertainty, and h_s is characteristic constant. The gravitational acceleration as a function of r is given by

$$g = \frac{\mu}{r^2} \quad (4)$$

where μ is gravitational constant.

3 Guidance Law Design

3.1 State Feedback Guidance Law Based on ISS

Due (2b), one has

$$\dot{D} = \frac{1}{2} \dot{\rho} v^2 C_D \frac{S}{m} + \rho v \dot{v} C_D \frac{S}{m} + \frac{1}{2} \rho v^2 \dot{C}_D \frac{S}{m} \quad (5)$$

and

$$\frac{\dot{D}}{D} = \frac{\dot{\rho}}{\rho} + \frac{2\dot{v}}{v} + \frac{\dot{C}_D}{C_D} \quad (6)$$

It can also be calculated out that

$$\frac{\dot{\rho}}{\rho} = -\frac{\dot{h}}{h_s} + \delta_\rho = -\frac{\dot{r}}{h_s} + \delta_\rho \stackrel{\text{Eq. (1a)}}{=} -\frac{v \sin \gamma}{h_s} + \delta_\rho \quad (7a)$$

$$\frac{\dot{C}_D}{C_D} = \frac{\dot{C}_D^0}{C_D^0} + \delta_{C_D} \quad (7b)$$

$$\dot{g} = -\frac{2\mu}{r^3} v \sin \gamma = -\frac{2gv \sin \gamma}{r} \quad (7c)$$

where $\delta_\rho = \frac{\rho \Delta \dot{\rho} - \dot{\rho} \Delta \rho}{\rho(\rho - \Delta \rho)}$ and $\delta_{C_D} = \frac{\Delta \dot{C}_D C_D^0 - \dot{C}_D \Delta C_D}{C_D^0(C_D^0 + \Delta C_D)}$. Thus,

$$\frac{\dot{D}}{D} = -\frac{v \sin \gamma}{h_s} - \frac{2D}{v} - \frac{2g \sin \gamma}{v} + \underbrace{\frac{\dot{C}_D^0}{C_D^0}}_C + \underbrace{\delta_\rho + \delta_{C_D}}_\delta \quad (8)$$

Furthermore,

$$\ddot{D} = f(D, t) + g_0(D, t)u + \Delta(D, t) \quad (9)$$

where

$$u = \cos \sigma \quad (10)$$

and

$$f = \left(-\frac{v \sin \gamma}{h_s} - \frac{4D}{v} - \frac{2g \sin \gamma}{v} + C \right) \left(-\frac{v \sin \gamma}{h_s} D - \frac{2D^2}{v} - \frac{2g \sin \gamma}{v} D + CD \right) \\ + D \left(\frac{D \sin \gamma + g}{h_s} + \frac{4g \sin^2 \gamma - 2g \cos^2 \gamma}{r} - \frac{2D^2 + 4Dg \sin \gamma + 2g^2 \sin^2 \gamma - 2g^2 \cos^2 \gamma}{v^2} + \frac{v^2 \cos^2 \gamma}{rh_s} + \dot{C} \right)$$

$$g_0 = -\left(\frac{v}{h_s} + \frac{2g}{v} \right) \frac{LD \cos \gamma}{v} \\ \Delta = \dot{\delta} D + \left(-\frac{2v \sin \gamma}{h_s} - \frac{2D^2}{v} - \frac{4D}{v} - \frac{4g \sin \gamma}{v} + C + CD + \delta D \right) \delta$$

Since the purpose of designing a guidance law is to make the drag acceleration D track its reference value D^* by modulating the bank angle σ , we define $\tilde{D} = D - D^*$ and $x = [x_1, x_2]^T = [\tilde{D}, \dot{\tilde{D}}]^T$. The drag dynamics for guidance law design is formulated as

$$\dot{x} = \begin{bmatrix} x_2 \\ f(D, t) - \ddot{D}^* \end{bmatrix} + \begin{bmatrix} 0 \\ g_0(D, t) \end{bmatrix} u + \begin{bmatrix} 0 \\ \Delta(D, t) \end{bmatrix} \quad (12)$$

Here, we assume that uncertainties δ and $\dot{\delta}$ are bounded, and in a reasonable flight domain of interest there exist positive constants l and d such that

$$|\Delta| \leq l|x_1| + d \quad (13)$$

holds. In practice, the flight path angle γ always satisfies $-90^\circ < \gamma < 90^\circ$. From this, clearly, g_0 is invertible. Regarding (12), we have the following theorem.

Theorem 1 *Consider the system (12). There exists a guidance law*

$$u = g_0^{-1} \left(-f + \ddot{D}^* - \frac{a}{\varepsilon_0^2} x_1 - \frac{b}{\varepsilon_0} x_2 \right) \quad (14)$$

with $a > 0$, $b > 0$ and $\varepsilon_0 > 0$, such that the closed-loop system is ISS with respect to d , and moreover, the influence of uncertainties on x can be made close to zero for sufficiently small ε_0 .

Proof. Substituting guidance law (14) into (12) yields

$$\dot{x} = \underbrace{\begin{bmatrix} 0 & 1 \\ -\frac{a}{\varepsilon_0^2} & -\frac{b}{\varepsilon_0} \end{bmatrix}}_F x + \underbrace{\begin{bmatrix} 0 \\ 1 \end{bmatrix}}_B \Delta \quad (15)$$

The change of variables

$$\zeta_1 = \frac{x_1}{\varepsilon_0}, \quad \zeta_2 = x_2 \quad (16)$$

brings (15) into the form

$$\varepsilon_0 \dot{\zeta} = \underbrace{\begin{bmatrix} 0 & 1 \\ -a & -b \end{bmatrix}}_{F_0} \zeta + \varepsilon_0 B \Delta \quad (17)$$

where $\zeta = [\zeta_1, \zeta_2]^T$ and F_0 is a Hurwitz matrix. The derivative of Lyapunov function

$$V(\zeta) = \zeta^T P_0 \zeta \quad (18)$$

where P_0 is the positive definite solution of the Lyapunov equation $P_0 F_0 + F_0^T P_0 = -I$, along the trajectories of system (17) is given by

$$\begin{aligned} \dot{V} &= -\frac{1}{\varepsilon_0} \|\zeta\|^2 + 2\zeta^T P_0 B \Delta \\ &\leq -\frac{1}{\varepsilon_0} \|\zeta\|^2 + 2\|\zeta\| \|P_0 B\| (\varepsilon_0 l |\zeta_1| + d) \end{aligned} \quad (19)$$

Substituting the inequalities

$$\zeta^T P_0 B d \leq \frac{1}{2} \|\zeta\|^2 + \frac{1}{2} \|P_0\|^2 \|B\|^2 d^2$$

$$\varepsilon_0 \|\zeta\| \|P_0 B\| l |\zeta_1| \leq \varepsilon_0 \|P_0 B\| l \|\zeta\|^2$$

into Eq. (19), we obtain

$$\dot{V} \leq - \underbrace{\left(\frac{1}{\varepsilon_0} - 1 - 2\varepsilon_0 \|P_0 B\| l \right)}_{\kappa(\varepsilon_0)} \|\zeta\|^2 + \|P_0\|^2 \|B\|^2 d^2 \quad (20)$$

The boundedness of l leads to the fact that $\kappa(\varepsilon_0) > 0$ for sufficiently small ε_0 , and in this case, since

$$\lambda_{\min}(P_0) \|\zeta\|^2 \leq V(\zeta) \leq \lambda_{\max}(P_0) \|\zeta\|^2 \quad (21)$$

we have

$$\|\zeta(t)\|^2 \leq \lambda_3 e^{-\lambda_1 t} \|\zeta(0)\|^2 + \frac{\lambda_2}{\lambda_1} (1 - e^{-\lambda_1 t}) d^2 \quad (22)$$

and

$$\|x(t)\| = \|\varphi(\varepsilon_0)\zeta(t)\| \leq \sqrt{\lambda_3 e^{-\lambda_1 t}} \|x(0)\| + \|\varphi(\varepsilon_0)\| \sqrt{\frac{\lambda_2}{\lambda_1}} d \quad (23)$$

where $\varphi(\varepsilon_0) = \text{diag}(\varepsilon_0, 1)$, $\lambda_1 = \frac{\kappa(\varepsilon_0)}{\lambda_{\max}(P_0)}$, $\lambda_2 = \frac{\|B\|^2 \|P_0\|^2}{\lambda_{\min}(P_0)}$, $\lambda_3 = \frac{\lambda_{\max}(P_0)}{\lambda_{\min}(P_0)}$. From Eq. (23), it can be seen that the closed-loop system is ISS with respect to d , and the influence of uncertainties on x will be close to zero for sufficiently small ε_0 .

□

If all the variables can be measured accurately, \dot{D} can be calculated from Eq. (8). However, there are always unknown uncertainties in atmospheric density and aerodynamic coefficients [1, 11], i.e., $\delta \neq 0$, which implies that the accurate information of \dot{D} is hard to get actually. The guidance law without drag rate measurement will be designed in next subsection by combining a high-gain observer with guidance law (14).

Remark 1 A similar result (ISS property of the close-loop system) has been got in [11] under the assumption that the uncertainties related term Δ is bounded. However, since Δ is also a function of \tilde{D} , strictly speaking, the boundedness of Δ cannot be guaranteed. Different from [11], we assume that $|\Delta|$ is not bigger than a linear function of $|\tilde{D}|$ as shown by (13) in a reasonable flight domain of interest, and a robust guidance law is also obtain based on ISS theory.

3.2 Guidance Law without Drag Rate

The guidance law without knowledge of drag rate can be got by replacing \hat{x}_2 instead of x_2 in (14), i.e.,

$$u = g_0^{-1} \left(-f + \ddot{D}^* - \frac{a}{\varepsilon_0^2} x_1 - \frac{b}{\varepsilon_0} \hat{x}_2 \right) \quad (24)$$

where \hat{x}_2 is the estimate of drag rate and generated by the high-gain observer

$$\dot{\hat{x}}_1 = \hat{x}_2 + \frac{l_1}{\varepsilon} (x_1 - \hat{x}_1) \quad (25a)$$

$$\dot{\hat{x}}_2 = -\frac{a}{\varepsilon_0^2} x_1 - \frac{b}{\varepsilon_0} \hat{x}_2 + \frac{l_2}{\varepsilon^2} (x_1 - \hat{x}_1) \quad (25b)$$

with $l_1 > 0$, $l_2 > 0$, $\varepsilon > 0$, and $\hat{x} = [\hat{x}_1, \hat{x}_2]^T$. The main results can be stated as the following theorem.

Theorem 2 *Consider the closed-loop system of system (12) and guidance law (24) with high-gain observer (25). Let $\tilde{x} = x - \hat{x}$. There exists a positive constant ε_1^* such that, for every $0 < \varepsilon < \varepsilon_1^*$, (x, \tilde{x}) is ISS with respect to d , and the uncertainties can be suppressed by adjusting ε and ε_0 . Besides, if d vanishes, there exists $\varepsilon_2^* > 0$ such that, for every $0 < \varepsilon < \varepsilon_2^*$, x and \tilde{x} can converge to zero exponentially.*

Proof. The change of variables

$$\eta_1 = \frac{\tilde{x}_1}{\varepsilon}, \quad \eta_2 = \tilde{x}_2 \quad (26)$$

bring the closed-loop system into the form

$$\dot{x} = Fx + B \left(\Delta + \frac{b}{\varepsilon_0} \eta_2 \right) \quad (27a)$$

$$\varepsilon \dot{\eta} = \underbrace{\begin{bmatrix} -l_1 & 1 \\ -l_2 & 0 \end{bmatrix}}_{A_0} \eta + \varepsilon B \Delta \quad (27b)$$

where $\eta = [\eta_1, \eta_2]^T$, F and B have been given in (15), and A_0 is a Hurwitz matrix. Transforming x to ζ by Eq. (16), we rewritten the closed-loop system as

$$\dot{\zeta} = \frac{1}{\varepsilon_0} F_0 \zeta + B \left(\Delta + \frac{b}{\varepsilon_0} \eta_2 \right) \quad (28a)$$

$$\dot{\eta} = \frac{1}{\varepsilon} A_0 \eta + B \Delta \quad (28b)$$

The derivative of Lyapunov function

$$V_{com}(\zeta, \eta) = V(\zeta) + \eta^T P \eta \quad (29)$$

where $V(\zeta)$ is defined by (18) and P is the positive definite solution of the Lyapunov equation

$PA_0 + A_0^T P = -I$, along the trajectories of system (28) is given by

$$\begin{aligned} \dot{V}_{com} &= -\frac{1}{\varepsilon_0} \|\zeta\|^2 + 2\zeta^T P_0 B \left(\Delta + \frac{b}{\varepsilon_0} \eta_2 \right) - \frac{1}{\varepsilon} \|\eta\|^2 + 2\eta^T P B \Delta \\ &\leq -\frac{1}{\varepsilon_0} \|\zeta\|^2 + 2\|\zeta\| \|P_0 B\| \left(\varepsilon_0 l |\zeta_1| + d + \frac{b}{\varepsilon_0} |\eta_2| \right) - \frac{1}{\varepsilon} \|\eta\|^2 + 2\|\eta\| \|P B\| (\varepsilon_0 l |\zeta_1| + d) \\ &\leq -\frac{1}{\varepsilon_0} \|\zeta\|^2 + 2\|\zeta\| \|P_0 B\| \left(\varepsilon_0 l \|\zeta\| + d + \frac{b}{\varepsilon_0} \|\eta\| \right) - \frac{1}{\varepsilon} \|\eta\|^2 + 2\|\eta\| \|P B\| (\varepsilon_0 l \|\zeta\| + d) \quad (30) \end{aligned}$$

Substituting the inequality

$$\|\zeta\| \|P_0 B\| d \leq \frac{1}{2} \|\zeta\|^2 + \frac{1}{2} \|P_0\|^2 \|B\|^2 d$$

$$\|\eta\| \|P B\| d \leq \frac{1}{2} \|\eta\|^2 + \frac{1}{2} \|P\|^2 \|B\|^2 d$$

yields

$$\begin{aligned}
\dot{V}_{com} &\leq - \underbrace{\left(\frac{1}{\varepsilon_0} - 1 - 2\varepsilon_0 \|P_0 B\| l \right)}_{\kappa(\varepsilon_0)} \|\zeta\|^2 - \left(\frac{1}{\varepsilon} - 1 \right) \|\eta\|^2 \\
&\quad + 2 \underbrace{\left(\frac{b}{\varepsilon_0} \|P_0 B\| + \varepsilon_0 l \|PB\| \right)}_{\alpha} \|\zeta\| \|\eta\| + \underbrace{(\|P_0\|^2 + \|P\|^2) \|B\|^2}_{C_0} d^2 \\
&= -\mathcal{X}^T Q \mathcal{X} + C_0 d^2
\end{aligned} \tag{32}$$

where

$$\mathcal{X} = \begin{bmatrix} \|\zeta\| \\ \|\eta\| \end{bmatrix}, \quad Q = \begin{bmatrix} \kappa(\varepsilon_0) & -\alpha \\ -\alpha & \frac{1}{\varepsilon} - 1 \end{bmatrix}$$

For bounded l and $\kappa(\varepsilon_0) > 0$, the matrix Q will be positive definite for sufficiently small ε . Hence,

there exists $\varepsilon_1^* > 0$ such that, for $0 < \varepsilon < \varepsilon_1^*$, we have $\lambda_{\min}(Q) > 0$, and the inequality

$$\dot{V}_{com} \leq -\lambda_{\min}(Q) \|\mathcal{X}\|^2 + C_0 d^2 \tag{33}$$

holds. Let $\mathcal{Y} = [\zeta, \eta]^T$. Since $\|\mathcal{X}\| = \|\mathcal{Y}\|$, we have

$$\lambda_{\min}(P') \|\mathcal{X}\|^2 = \lambda_{\min}(P') \|\mathcal{Y}\|^2 \leq V_{com} = \mathcal{Y}^T P' \mathcal{Y} \leq \lambda_{\max}(P') \|\mathcal{Y}\|^2 = \lambda_{\max}(P') \|\mathcal{X}\|^2 \tag{34}$$

where $P' = \text{block diag}\{\frac{1}{2}I_2, P_0\}$. Substituting Eq. (34) into Eq. (33) yields

$$\dot{V}_{com} \leq -\frac{\lambda_{\min}(Q)}{\lambda_{\max}(P')} V_{com} + C_0 d^2 \tag{35}$$

that is

$$V_{com}(\mathcal{Y}(t)) \leq e^{-\lambda_1 t} V_{com}(\mathcal{Y}(0)) + \frac{C_0}{\lambda_1} (1 - e^{-\lambda_1 t}) d^2 \tag{36}$$

where $\lambda_1 = \frac{\lambda_{\min}(Q)}{\lambda_{\max}(P')}$. Substituting Eq. (34) into Eq. (36), we have

$$\|\mathcal{Y}(t)\|^2 \leq \lambda_2 e^{-\lambda_1 t} \|\mathcal{Y}(0)\|^2 + \frac{C_0}{\lambda_1 \lambda_3} (1 - e^{-\lambda_1 t}) d^2 \tag{37}$$

where $\lambda_2 = \frac{\lambda_{\max}(P')}{\lambda_{\min}(P')}$, $\lambda_3 = \lambda_{\min}(P')$. Therefore, $\mathcal{Y}(t)$ satisfies

$$\|\mathcal{Y}(t)\| \leq \sqrt{\lambda_2 e^{-\lambda_1 t}} \|\mathcal{Y}(0)\| + \sqrt{\frac{C_0}{\lambda_1 \lambda_3}} (1 - e^{-\lambda_1 t}) d \quad (38)$$

Therefore, system (28) is ISS with respect to d for $0 < \varepsilon \leq \varepsilon_1^*$. λ_1 can be sufficiently large by adjusting ε_0 and ε , and, accordingly, it can be seen from Eq. (38) that the uncertainties can be suppressed.

Moreover, if d vanishes, (38) can be rewritten as $\|\mathcal{Y}(t)\| \leq \sqrt{\lambda_2 e^{-\lambda_1 t}} \|\mathcal{Y}(0)\|$, where $\lambda_1 > 0$ for sufficiently small ε . Therefore, there exists $\varepsilon_2^* > 0$ such that, for every $0 < \varepsilon \leq \varepsilon_2^*$, the origin of system (28) is exponentially stable.

The proof is completed. □

Remark 2 Actually, $u = \cos \sigma$ is bounded by ± 1 , but the control saturation problem is not considered in this paper since it is implicitly assumed that the vehicle has enough maneuvering capacity to achieve drag-tracking in reasonable cases by modulating the bank angle magnitude ($0^\circ \leq \sigma \leq 180^\circ$). Guidance law design with measurable information for entry subject to control saturation will be investigated in the future work.

4 Simulation Results

This section presents simulation results to test the performance of the proposed guidance laws.

Consider the Mars atmospheric entry flight, and vehicle, reference drag profile and other data from [1] are used. The Mars lander has surface area of 16m^2 and weighs 992kg [18]. The lift-to-drag ratio and the ballistic coefficient are 0.18 and 115kg/m^2 , respectively. The initial

and final state variables can be found in Table 1. It can be calculated out that the desired total downrange is 723.32km.

Fist, the performance of guidance law (14) is tested with taking $\varepsilon_0 = 5, a = 1.982, b = 3$, and the simulation results are shown in Figs. 1-5. It is can be seen that the reference profiles can be well tracked under the guidance law, and the downrange error is 0.00475km. Then, guidance law (24) with observer (25) is used for $\varepsilon_0 = 5, a = 1.982, b = 3, l_1 = 2l_2 = 2, \varepsilon = 0.481$, and the simulation results are shown in Figs. 6-10. Comparing with Figs. 1-5, we can see that the performance of guidance law (14) can be recovered by using the high-gain observer with sufficiently small ε , and the downrange error is 0.0722km. Since the atmospheric density is very small at the beginning of entry and it leads to the fact that $g_0(D, t) = -\left(\frac{v}{h_s} + \frac{2q}{v}\right) \frac{LD \cos \gamma}{v}$ is small, thus, a large control magnitude is needed to make the drag track its reference value, which is the reason why bank angle reaches saturation level at initial time with both guidance laws.

Table 1: State Variables

Initial State Variables		Final State Variables	
Altitude, h_0 (km)	126.1	Altitude, h_f (km)	10
Relative velocity, V_0 (km/s)	6.75	Relative Velocity, V_f (m/s)	503
Flight path angle, γ_0 (°)	-14.4	Flight path angle, γ_f (°)	—
Longitude (°)	0	Longitude (°)	12.2
Latitude (°)	0	Latitude (°)	0

To test the robustness of the proposed guidance law (24) with observer (25), a 1000-run Monte Carlo study using the parameter deviation in Table 2 is done. Take $\varepsilon_0 = 20, a = 20, b =$

Table 2: Statistics of Dispersions Used in Monte Carlo Study

Parameters	Distribution	$[\Delta^-, \Delta^+]$
Mass deviation	uniform	[-5%,5%]
Atmospheric density deviation	uniform	[-20%,20%]
C_L deviation	uniform	[-30%,30%]
C_D deviation	uniform	[-30%,30%]

Table 3: Result of Monte Carlo Study

	Downrange Error (km)	Altitude Error (km)
Minimum	0.0028	-0.0013
Maximum	24.3249	3.9263
Average	2.3957	0.6369
Standard deviation	6.7809	0.8584

$5, l_1 = 2l_2 = 2, \varepsilon = 0.45$, and the result is shown in Fig. 11. We can see that most of the downrange errors can be kept between -10km and 20km, while the altitude errors are kept between -0.6km and 4km. The result of this Monte Carlo study is summarized in Table 3.

5 Conclusions

A nonlinear drag-tracking guidance law was designed based on input-to-state stability (ISS) and a high-gain observer for entry vehicles. The proposed approach does not require prior information of drag rate, and it was proven that the drag-tracking error is ISS with respect

to the uncertainties by using the guidance law with a sufficiently fast high-gain observer. The stability analysis as well as the simulation results show that the scheme can be effectively used in entry phase.

Acknowledgments

The authors would like to thank Dr. Minwen Guo for her help in simulation study, and Dr. Xinghu Wang for his comments on this paper.

References

- [1] D. Y. Wang and M. W. Guo, Robust guidance law for drag tracking in mars atmospheric entry flight, Proceedings of the 33rd Chinese Control Conference, Nanjing, China, 2014, pp. 697-702.
- [2] A. Saraf, A. Leavitt, D. T. Chen, et al. Design and evaluation of an acceleration guidance algorithm for entry, Journal of Spacecraft and Rockets, 2004, Vol. 41, No. 6, 2004, pp. 986-996.
- [3] J. C. Harpold and C. A. Graves, Shuttle entry guidance, Journal of the Astronautical Sciences, Vol. 27, No. 3, 1979, pp. 239-268.
- [4] K. D. Mease, D. T. Chen, P. Teufel, et al. Reduced-order entry trajectory planning for acceleration guidance, Journal of Guidance, Control and Dynamics, 2002, Vol. 25, No. 2, 2002, pp. 257-266.

- [5] J. A. Leavitt, K. D. Mease, Feasible trajectory generation for atmospheric entry guidance, *Journal of Guidance, Control and Dynamics*, Vol. 30, No. 2, 2007 pp. 472-481.
- [6] S. H. Wang, P. L. Fei, X. X. Liu and B. Zhang, A new evolved acceleration reentry guidance for reusable launch vehicles, *Applied Mechanics and Materials*, Vols. 380-384, 2013, pp. 576-580.
- [7] S. E. Talole, J. Benito and K. D. Mease, Sliding mode observer for drag tracking in entry guidance, *Proceedings of the AIAA Guidance, Navigation and Control Conference*, Hilton Head, South Carolina, 2007, pp. 5122-5137.
- [8] P. Lu, Nonlinear Predictive controllers for continuous systems, *Journal of Guidance, Control and Dynamics*, Vol. 17, No. 3, 1994, pp. 553-560.
- [9] P. Lu, Entry guidance and trajectory control for reusable launch vehicle, *Journal of Guidance, Control and Dynamics*, Vol. 20, No. 1, 1997, pp. 143-149.
- [10] J. Benito and K. D. Mease, Nonlinear predictive controller for drag tracking in entry guidance, *Proceedings of the 2008 AIAA/AAS Astrodynamics Specialist Conference and Exhibit*, Honolulu, Hawaii, AIAA-2008-7350.
- [11] M. W. Guo and D. Y. Wang, Guidance laws for low-lifting skip reentry subject to control saturation based on nonlinear predictive control, *Aerospace Science and Technology*, doi:10.1016/j.ast.2014.05.004.
- [12] M. W. Spong, On the robust control of robot manipulators, *IEEE Transactions on Automatic Control*, Vol. 37, 1992, pp. 1782-1786.

- [13] R. F. Chen, Y. Q. Xia, Drag-based entry guidance for mars pinpoint landing, Proceedings of the 32nd Chinese Control Conference, Xi'an, China, 2013, pp. 5473-5478.
- [14] B. L. Tian and Q. Zong, Optimal guidance for reentry vehicle based on indirect Legendre pseudospectral method, Acta Astronautica, Vol. 68, No. 7-8, 2011, pp. 1176-1184.
- [15] F. Esfandiari and H. K. Khalil, Output feedback stabilization of fully linearizable systems, International Journal of Control, Vol. 56, No. 5, 1992, pp. 1007-1037.
- [16] A. N. Atassi and H. K. Khalil, A separation principle for the stabilization of a class of nonlinear systems, IEEE Transactions on Automatic Control, Vol. 44, No. 9, 1999, pp. 1672-1687.
- [17] H. K. Khalil, Nonlinear systems, 3rd ed., Prentice-Hall, Upper Saddle River, NJ, 2002, Chap. 4.
- [18] H. J. Shen, H. Seywald and R. W. Powell, Desensitizing the pin-point landing trajectory on Mars, Proceedings of the AIAA/AAS Astrodynamics Specialist Conference and Exhibit, Honolulu, Hawaii, 2008.

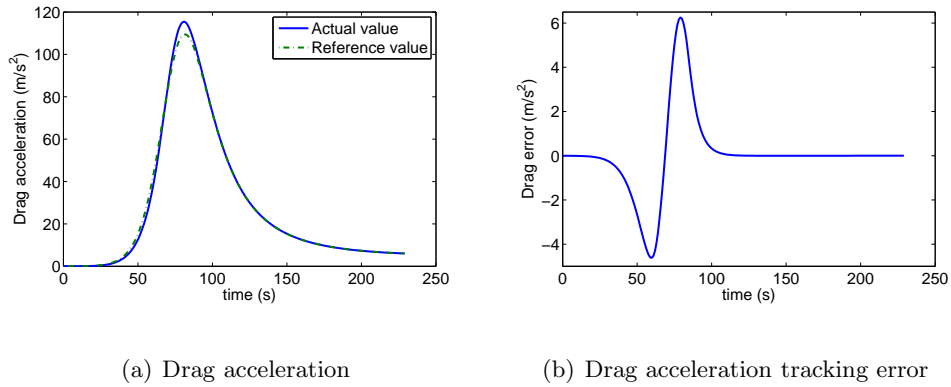
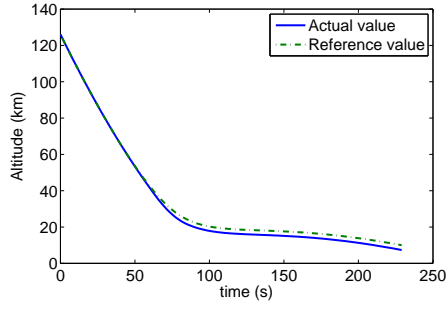
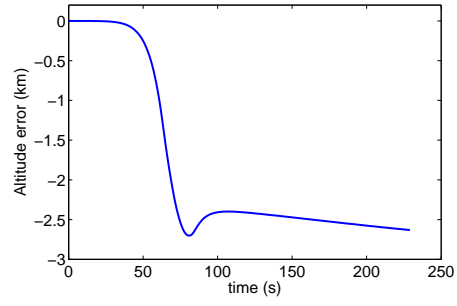


Figure 1: Drag tracking with state feedback guidance law (14)

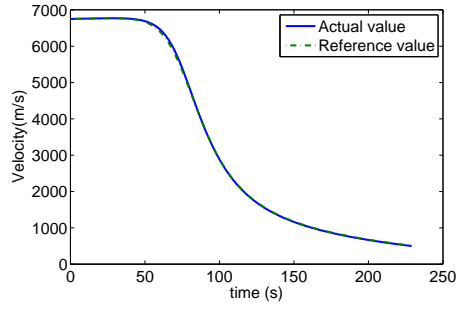


(a) Altitude

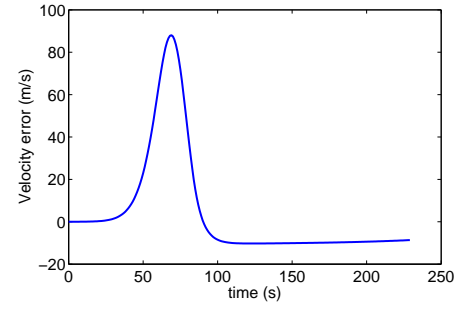


(b) Altitude tracking error

Figure 2: Altitude tracking with state feedback guidance law (14)

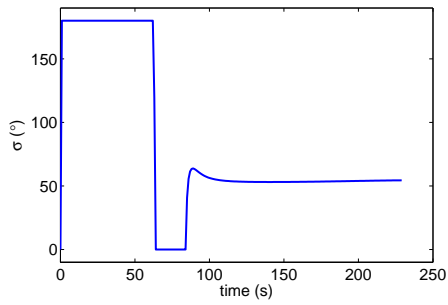


(a) Velocity

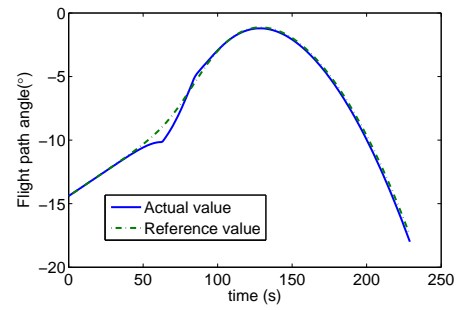


(b) Velocity tracking error

Figure 3: Velocity tracking with state feedback guidance law (14)



(a) σ



(b) γ

Figure 4: Bank angle and flight path angel with state feedback guidance law (14)

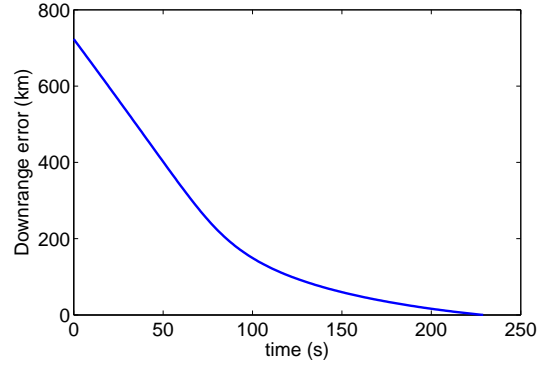
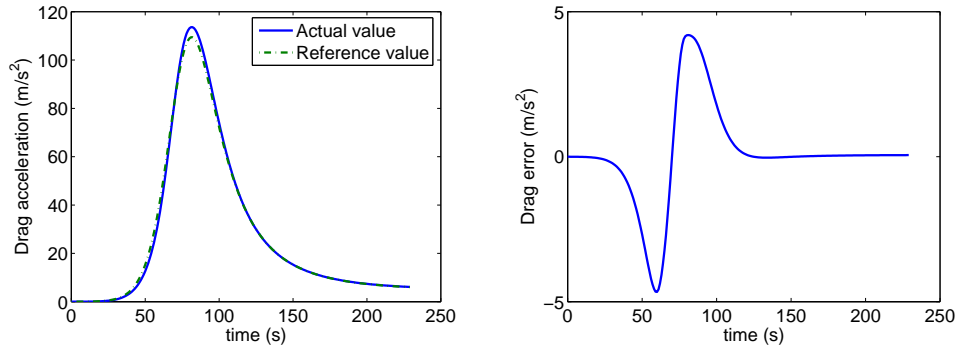


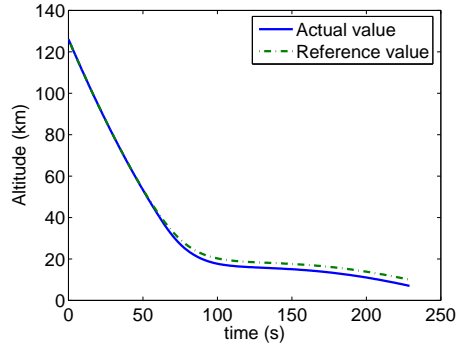
Figure 5: Downrange error with state feedback guidance law (14)



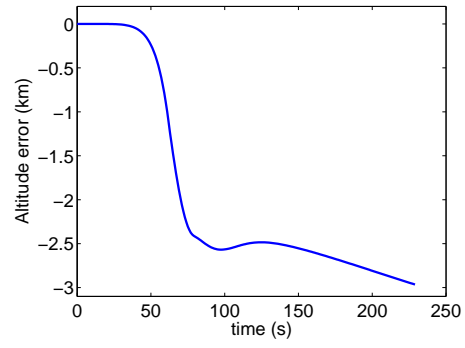
(a) Drag acceleration

(b) Drag acceleration tracking error

Figure 6: Drag tracking with guidance law (24) with observer (25)

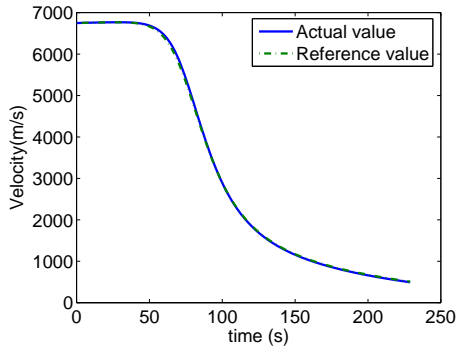


(a) Altitude

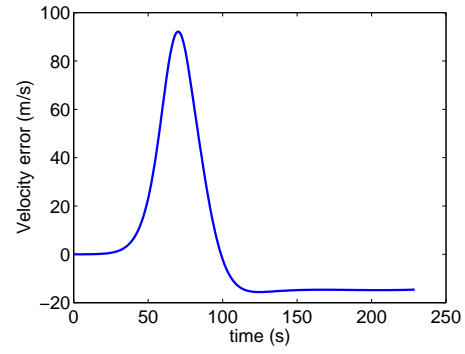


(b) Altitude tracking error

Figure 7: Altitude tracking with guidance law (24) with observer (25)

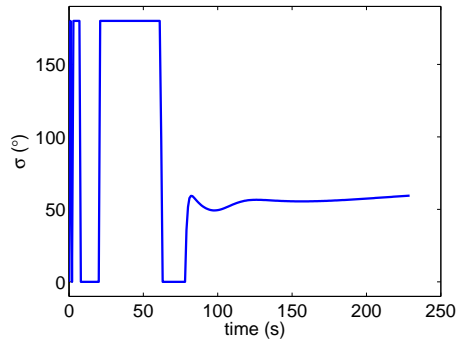


(a) Velocity

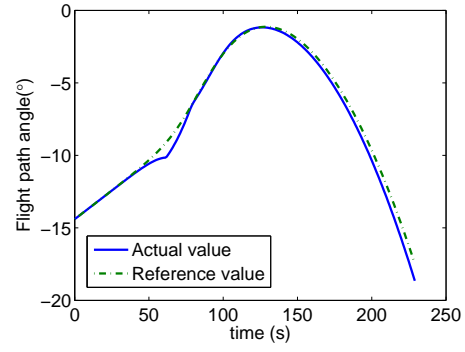


(b) Velocity tracking error

Figure 8: Velocity tracking with guidance law (24) with observer (25)

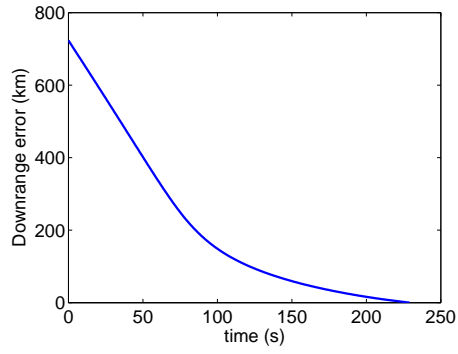


(a) σ

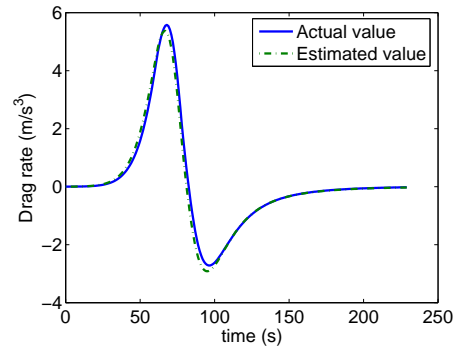


(b) γ

Figure 9: Bank angle and flight path angel with guidance law (24) with observer (25)

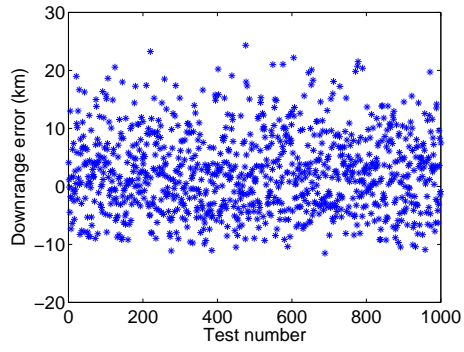


(a) Downrange error

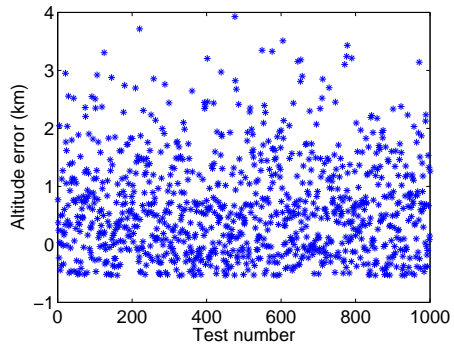


(b) Drag rate

Figure 10: Downrange error and drag rate with guidance law (24) with observer (25)



(a) Downrange error



(b) Altitude error

Figure 11: Monte Carlo study of guidance law (24) with observer (25)